Decoupling degradation in exciton formation and recombination during lifetime testing of organic light-emitting devices

Cite as: Appl. Phys. Lett. **111**, 113301 (2017); https://doi.org/10.1063/1.4993618
Submitted: 29 June 2017 . Accepted: 31 August 2017 . Published Online: 14 September 2017

Kyle W. Hershey, John Suddard-Bangsund, Gang Qian, and Russell J. Holmes

Decoupling degradation in exciton formation and recombination during lifetime testing of organic light-emitting devices

Kyle W. Hershey, John Suddard-Bangsund, Gang Qian, and Russell J. Holmes
Department of Chemical Engineering and Materials Science, University of Minnesota, Minneapolis, Minnesota 55455, USA

(Received 29 June 2017; accepted 31 August 2017; published online 14 September 2017)

The analysis of organic light-emitting device degradation is typically restricted to fitting the overall luminance loss as a function of time or the characterization of fully degraded devices. To develop a more complete understanding of degradation, additional specific data are needed as a function of luminance loss. The overall degradation in luminance during testing can be decoupled into a loss in emitter photoluminescence efficiency and a reduction in the exciton formation efficiency. Here, we demonstrate a method that permits separation of these component efficiencies, yielding the time evolution of two additional specific device parameters that can be used in interpreting and modeling degradation without modification to the device architecture or introduction of any additional post-degradation characterization steps. Here, devices based on the phosphor tris[2-phenylpyridinato-C^2,N]iridium(III) ($Ir(ppy)_3$) are characterized as a function of initial luminance and emissive layer thickness. The overall loss in device luminance is found to originate primarily from a reduction in the exciton formation efficiency which is exacerbated in devices with thinner emissive layers. Interestingly, the contribution to overall degradation from a reduction in the efficiency of exciton recombination (i.e., photoluminescence) is unaffected by thickness, suggesting a fixed exciton recombination zone width and degradation at an interface. *Published by AIP Publishing.*
[http://dx.doi.org/10.1063/1.4993618]

Operational lifetime is one of the most critical metrics defining organic light-emitting device (OLED) performance.[1–8] Frequently, OLED degradation is characterized by a reduction in device electroluminescence (EL) intensity (luminance) or an increase in device driving voltage with time at a fixed current density. The device lifetime is then reported as the time over which some arbitrary fraction of the initial luminance is lost. While useful in comparing the relative stability of different devices, this approach does not typically provide insight into specific degradation mechanisms. Often, additional chemical, structural, or spectroscopic analysis is needed in order to identify molecular degradation pathways or changes in interface quality and film morphology.[4,9–13] Attempts to quantitatively model the luminance decay have sought to provide a mechanistic form for the degradation pathways.[14–17] While these efforts have offered new insights into the cause of luminance loss, detailed analysis can be challenging due to model overparameterization with limited experimental data. With existing techniques for probing OLED luminance loss, it is challenging to inform material and device design due to the ambiguity and complexity surrounding device degradation. Additional sources of data regarding the degradation are needed to enhance modeling efforts and ultimately guide material and device design. Here, the overall degradation in luminance efficiency is considered in terms of the component efficiencies of exciton recombination (i.e., emitter photoluminescence efficiency) and exciton formation. This work introduces a technique to separately isolate the degradation of these component efficiencies using a single measurement of device luminance versus time. While the reduction in the photoluminescence (PL) intensity has been previously reported as a function of overall EL degradation,[18–20] this work offers additional valuable insight by fully decoupling contributions to the overall degradation from losses in the efficiency of exciton formation and recombination.

Under constant current density excitation, a reduction in device EL can be attributed to a decrease in the device external quantum efficiency (η_{EQE}), which can be expressed as

$$\eta_{EQE} = \eta_{PL}\eta_{OC}\chi\eta_{EF}\eta_{\tau}, \tag{1}$$

where η_{PL} is the PL efficiency of the emissive layer, η_{OC} is the optical out-coupling efficiency, χ is the exciton spin fraction, defining the fraction of excitons permitted to radiatively recombine, and η_{EF} is the efficiency of exciton formation on the emitter. Competing with exciton formation are charge carrier losses captured in the charge balance factor,[21] as well as additional carrier recombination losses via the formation of non-radiative recombination centers.[22,23] The term η_{τ} is the current density-dependent fraction of excitons that relax by natural recombination defined by the lifetime, τ. This is a modification to the traditional decomposition of η_{EQE},[24] accounting for excitons lost to bimolecular quenching. For the preliminary discussion, we assume η_{τ} is constant during device degradation, but revisit this approximation at the end of this work. Since the reduction in device luminance with time reflects a reduction in η_{EQE}, Eq. (1) can be used to isolate the various contributions to overall luminance loss. In the absence of large scale crystallization, η_{OC} is not expected to change during degradation. While a change in recombination zone position could also change η_{OC}, this effect is expected to be small for thin emissive layers. In the absence of new emission features, χ is assumed to be constant during

testing. Therefore, the ratio of the degraded external quantum efficiency at some time, t, ($\eta_{EQE}(t)$) to the initial efficiency (η^0_{EQE}) can be expressed as

$$\frac{\eta_{EQE}(t)}{\eta^0_{EQE}} = \frac{\eta_{PL}(t)}{\eta^0_{PL}} \frac{\eta_{EF}(t)}{{\eta_{EF}}^0}. \tag{2}$$

The ratio of η_{EQE} on the left of Eq. (2) is experimentally measured during device degradation as the change in EL (or luminance). The change in PL intensity during degradation can also be measured on the same device by intermittently exciting the device optically and collecting the resulting luminance.[22,25] The relative change in PL intensity ($L_{PL}(t)/L^0_{PL}$) can be related to the PL efficiency ratio in Eq. (2) as

$$\frac{\eta_{PL}(t)}{\eta^0_{PL}} = \frac{L_{PL}(t)}{L^0_{PL}} \frac{I^0}{I(t)}, \tag{3}$$

where I is the optical pump intensity absorbed by the emissive layer. Depending on the choice of active materials, the wavelength of the optical pump can be chosen to excite only the luminescent guest in a host-guest device. If the absorption coefficient of the emissive layer remains constant during device degradation, the PL efficiency ratio is directly proportional to the PL intensity ratio. Thus, with a measurement of emissive layer PL intensity (and hence η_{PL}) during degradation, the reduction in the exciton formation efficiency may also be extracted. In this way, degradation in both the exciton recombination and formation efficiencies is known for the device. This decoupling assumes that the optical absorption and recombination zone profiles overlap significantly so that the same guest emissive molecules are probed under optical and electrical excitation. For devices with thick recombination zones or highly asymmetric recombination zone profiles, this approximation may need to be considered more rigorously.

In a typical measurement of OLED degradation, EL is collected as a function of time under a fixed driving current density that corresponds to a desired initial luminance. To continuously collect device PL in addition to EL, the current source is disabled every 10 min and a 1 mm diameter circular spot on the device is excited by a continuous-wave laser at a wavelength of $\lambda = 405$ nm ($\sim$10 mW/cm^2). For the devices considered in this study, this pump wavelength excites only the luminescent guest species in the emissive layer (EML). The experimental configuration is shown in Fig. 1(a) with the electrical-optical excitation scheme shown in Fig. 1(b). The laser is incident on the device for $\sim$5 s to ensure sufficient time for averaging of the resulting PL signal. The laser intensity is kept low enough so that no degradation is observed during averaging.[26] After PL collection, electrical excitation is resumed. Operational time is recorded based on the time under electrical excitation, with the time for PL measurements excluded. This excitation scheme yields lifetimes consistent with uninterrupted electrical excitation measurements of the same architecture.

Organic light-emitting devices were fabricated on glass substrates pre-patterned with indium-tin-oxide (ITO). After cleaning with solvents and UV ozone ambient, organic layers were deposited using vacuum thermal sublimation. The device

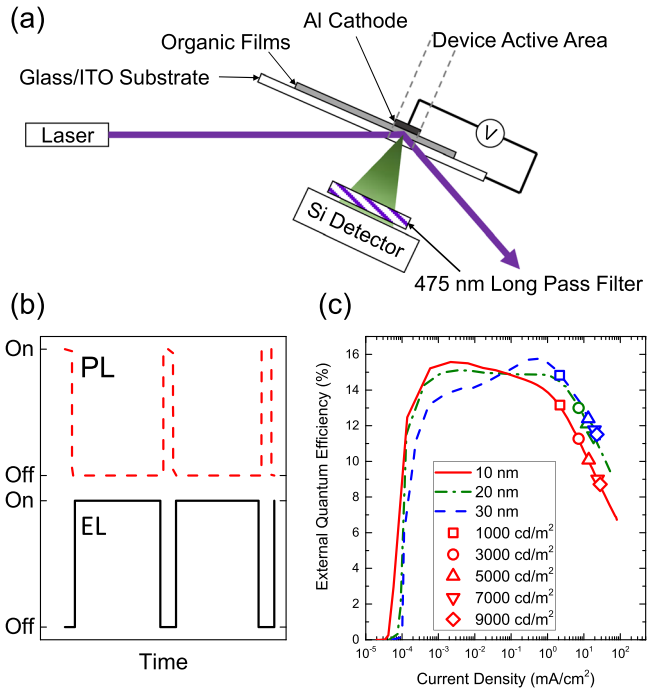

FIG. 1. (a) Experimental configuration for the measurement of electro- (EL) and photoluminescence (PL) during OLED degradation. Laser excitation is incident on a subsection of the device area. The laser is aligned so that neither the incident nor reflected beam strikes the detector. Stray laser light is removed by a $\lambda = 475$ nm dielectric long pass filter. (b) Excitation scheme. EL and PL signals are probed independently with no temporal overlap. (c) External quantum efficiency versus current density and luminance for devices having emissive layer thicknesses of 10 nm, 20 nm, and 30 nm.

active area is a 0.25 cm^2. After layer deposition, devices were encapsulated in a N_2 glovebox using glass cover slides and UV cured epoxy surrounding the device area. Devices consisted of a 60-nm-thick hole-injection layer of Plexcore AQ1200 spin-cast on a glass substrate coated with a 150-nm-thick layer of indium-tin-oxide (ITO), followed by a 30-nm-thick hole-transport layer of *N*,*N*′-bis(naphthalen-1-yl)-*N*,*N*′-bis(phenyl)-benzidine (NPD), and an EML of 4,4′-bis(*N*-carbazolyl)-1,1′-biphenyl (CBP) doped at 6 vol. % with tris[2-phenylpyridinato-C^2,N]iridium(III) (Ir(ppy)$_3$). The emissive layer was capped with a 10-nm-thick layer of 2,2′,2″-(1,3,5-benzinetriyl)-tris(1-phenyl-1-H-benzimidazole) (TPBi), and a 30-nm-thick layer of tris-(8-hydroxyquinoline)aluminum (Alq$_3$). The cathode for each device consisted of a 0.5-nm-thick layer of LiF and a 100-nm-thick layer of Al. Champion devices showed peak external quantum efficiencies of $\eta_{EQE} = 15.7\%$, 15.3%, and 15.7%, for devices with EML thicknesses of 10, 20, and 30 nm, respectively, as shown in Fig. 1(c). Equation (2) requires that η_{OC} remains constant during device degradation. Indeed, no birefringence was observed under cross-polarization before or after degradation, suggesting the absence of large-scale crystallization. Further, no new emission features were detected as a function of device degradation. In devices having an EML thickness of 20 nm or 30 nm, the recombination zone position was characterized by doping a 3-nm-thick strip of the emissive layer either at the NPD/EML or TPBi/EML interface with an additional 1 vol. % of the quenching sensitizer tetraphenyl-tetrabenzoporphine (TPTBP). This technique has been previously used for assessing recombination zone width by quenching emission from

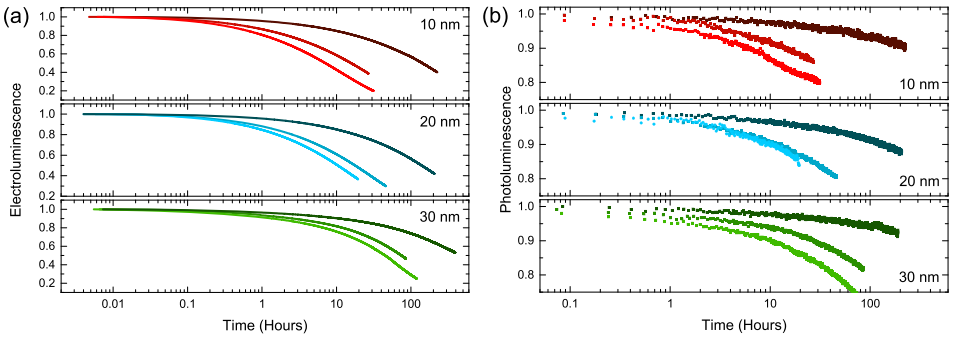

FIG. 2. Device decay curves for multiple values of the initial luminance as a function of emissive layer thickness. Loss in (a) electroluminescence (EL) and (b) photoluminescence (PL) are shown and decrease monotonically with increasing luminance. For devices with a 10-nm-thick emissive layer, initial luminance values are 1000 cd/m^2, 5000 cd/m^2, and 7000 cd/m^2. For devices with a 20-nm- or 30-nm-thick emissive layer, initial luminance values are 1000 cd/m^2, 5000 cd/m^2, and 7100 cd/m^2.

$Ir(ppy)_3$ while not significantly impacting the current density-voltage characteristics.[27] For devices with a 10-nm-thick EML, a 2-nm-thick strip of 0.5 vol. % platinum tetraphenyl-tetrabenzoporphine (PtTPTBP)[28] was used as an emissive sensitizer, again not impacting the current density-voltage characteristics.

Normalized EL and PL decays are shown in Figs. 2(a) and 2(b), respectively, for multiple initial device luminances and EML thicknesses, with testing conditions summarized in Table I. While a reduction in the EL lifetime is observed in Figs. 2 and 3 in reducing device thickness from 30 nm to 20 nm, little difference is seen between devices having EML thicknesses of 20 nm and 10 nm. The degradation in PL intensity does not appear to be a strong function of EML thickness. Indeed, comparing the EL and PL lifetimes with the extracted degradation in exciton formation (Figs. 2 and 3) shows that the EL decay is dominated by a loss in the efficiency of exciton formation with η_{EF} reaching 60% of its initial value (t_{60}) by the time EL has reached 50% (t_{50}). A substantial component of this decay may reflect the formation of non-radiative charge carrier recombination centers.[22,23] Over this same period, the PL intensity has only degraded by ~10% of its initial value.

The similarity in PL degradation observed across all EML thicknesses suggests that the exciton and polaron densities are similar between these devices,[15,29,30] and thus have similar exciton recombination zone widths. The accelerated degradation in the exciton formation efficiency (η_{EF}) observed for devices with EML thicknesses of 10 nm and 20 nm may indicate the presence of the recombination zone near the EML/TPBi interface, a configuration which has been previously shown to cause degradation.[31,32] To investigate this hypothesis, the position of the recombination zone was probed in devices with EML thicknesses of 20 and 30 nm using a quenching TPTBP sensitizer. The position of the recombination zone can be inferred by the corresponding reduction in device η_{EQE} due to quenching by TPTBP.[27] The sensitized 30-nm-thick EML devices showed no quenching, suggesting no recombination near the interface, while devices with a 20-nm-thick EML showed quenching only at the EML/TPBi interface, confirming the position of the recombination zone at that interface. Devices with a 10-nm-thick EML exhibited a change in current-voltage behavior when sensitized with TPTBP, and thus Pt-TPTBP, an emissive sensitizer with a peak wavelength of 770 nm, was used in 2-nm-thick strips on either side of the EML at 0.5 vol. %. This configuration matched the current-voltage behavior of the control device while permitting the measurement of emission from Pt-TPTBP. For devices with a 10-nm-thick EML, strong emission from Pt-TPTBP is observed from the EML/TPBi interface and weak emission is seen from the EML/NPD interface. These results suggest that for devices with an EML thickness of 10 nm or 20 nm, the recombination zone samples the EML/TPBi interface, accelerating exciton formation loss. While detailed analysis of the relevant degradation mechanism is the subject of future work, previous

TABLE I. Summary of device lifetimes for each device, the starting luminance (L_0), current density (J), starting voltage (V_0), and time at which 50% of the initial luminance is reached are shown.

d_{EML} (nm)	L_0 (cd/m^2)	J (mA/cm^2)	V_0 (V)	t_{50} (hours)
10	1000	2.2	4.2	139
	3000	7.2	5.1	39.9
	5000	13.6	5.4	15.8
	7000	14.4	6.2	6.9
	9000	28.0	6.3	5.3
20	1000	2.2	5.4	141.1
	3000	7.2	6.0	33.1
	5000	12.4	7.2	17.2
	7100	19.2	7.3	10.0
	9000	24.0	7.5	8.0
30	1000	2.2	5.9	474
	5000	13.6	7.3	74.4
	7100	19.6	7.6	46
	8000	22.4	7.7	38.1

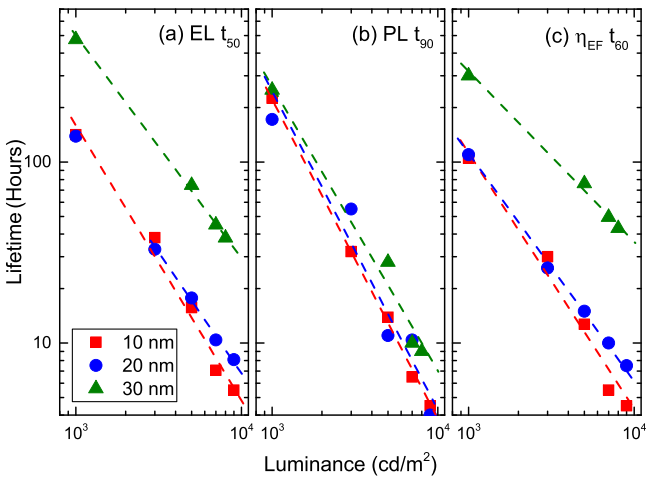

FIG. 3. (a) Electroluminescence t_{50}, (b) photoluminescence t_{90} (PL), and (c) exciton formation efficiency (η_{EF}) t_{60} as a function of initial luminance and emissive layer thickness.

work has suggested a role played by exciton-polaron interactions.[12,13,15,22,23]

The decoupling shown in Fig. 3 relies on being able to correlate the measured PL intensity to the η_{PL} of the emitter. Based on Eq. (3), a reduction in device PL with degradation may occur either as a loss in emitter absorption or a reduction in η_{PL}. If the reduction in η_{PL} is assumed to be due to an increase in the non-radiative exciton decay rate, k_{nr}, then the exciton lifetime ratio, $(\tau(t)/\tau^0)$ is directly proportional to (η_{PL}/η^0_{PL}). To extract the exciton lifetime, transient PL decays were collected by pumping the sample at $\lambda = 400$ nm using a N_2 dye laser with 1 ns pulses. The resulting emission was captured using an avalanche photodetector connected to an oscilloscope. At low exciton densities where single exponential decay is observed, undegraded devices show an exciton lifetime of (0.64 ± 0.03) μs with shorter lifetimes observed for degraded devices. As shown in Fig. 4, a 1:1 relationship is observed between the transient lifetime ratio and the PL ratio, showing that the degradation in PL comes exclusively from a loss in η_{PL}. Thus, a measurement of the PL intensity ratio can be treated as the PL efficiency ratio in Eq. (2). It is important to note that if a reduction in absorption was observed, the change could be characterized as a function of degradation, still allowing the extraction of the PL efficiency ratio.

An important aspect ignored in the analysis so far is the assumption that the fraction of excitons that suffer bimolecular quenching is fixed during the degradation measurement [i.e., $1-\eta_\tau$ in Eq. (1)]. During degradation, the exciton population decreases linearly with the luminance loss, likely causing an increase in η_τ. This would require the inclusion of an additional term of $\eta_\tau(t)/\eta^0_\tau$ in Eq. (2). Due to this modification, the reduction in the exciton formation efficiency, η_{EF}, would serve as an upper limit to the loss for constant η_τ. Using a previously developed model and measured rate constants,[21] along with a fixed polaron population and a recombination zone width of 10 nm, less than a 5% reduction in the reported exciton formation efficiency at t_{50} is expected in our regime of operation. This may actually overestimate the error since the polaron population likely increases as the exciton formation efficiency degrades.

The additional information offered by this technique is directed at improving the screening of active materials and device architectures for the realization of long-lived OLEDs. Device degradation that is dominated by a loss in either η_{EF} or η_{PL} implies a dominant rate process and an opportunity for improvement of materials or architecture. In systems using $Ir(ppy)_3$, a relatively stable emitter with demonstrated long optical and electrical lifetimes,[1,33] losses in the exciton formation efficiency are expected to represent the majority fraction of degradation. However, for novel molecules, limiting processes are largely unknown and would benefit from the separation of emitter and exciton formation efficiency loss. PL degradation could become increasingly important for blue-emitting species where the high exciton energies could contribute to material degradation.[1,34–38] This screening process would be dramatically improved if η_{EF} and η_{PL} can be mechanistically modeled. With additional datasets, modeling and understanding of degradation mechanisms can be improved and help to identify limiting processes.

In summary, this work presents a method for decoupling optical and electrical losses during OLED operational decay by attributing the overall reduction in electroluminescence to a loss in η_{PL} or the exciton formation efficiency (η_{EF}). Model devices are shown as a function of luminance, with a loss in η_{EF} shown to be the limiting factor. This technique allows access to additional experimental information which can offer insight about the degradation mechanism and understanding of device luminance loss. This added information can be used to aid future efforts in modeling degradation.

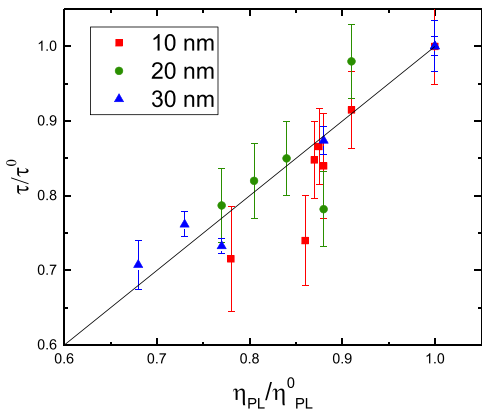

FIG. 4. Exciton lifetime ratio extracted from transient PL measurements on degraded and undegraded devices as a function of PL degradation ratio for several emissive layer thicknesses.

This work was supported by The Dow Chemical Company. J.S.B. acknowledges support from the National Science Foundation Graduate Research Fellowship under Grant No. 00039202. The authors acknowledge useful discussions with Dr. D. Wayne Blaylock and Dr. Peter Trefonas. R.J.H. is a member of The Dow Chemical Company Technical Advisory Board.

[1]S. Scholz, D. Y. Kondakov, B. Lüssem, and K. Leo, Chem. Rev. **115**, 8449 (2015).
[2]H. Aziz, Science **283**, 1900 (1999).
[3]H. Aziz, Z. Popovic, C. P. Tripp, N. X. Hu, A. M. Hor, and G. Xu, Appl. Phys. Lett. **72**, 2642 (1998).
[4]R. Seifert, I. Rabelo De Moraes, S. Scholz, M. C. Gather, B. Lüssem, and K. Leo, Org. Electron. Phys. Mater. Appl. **14**, 115 (2013).
[5]I. R. de Moraes, S. Scholz, B. Lüssem, and K. Leo, Appl. Phys. Lett. **99**, 53302 (2011).
[6]P. E. Burrows, V. Bulovic, S. R. Forrest, L. S. Sapochak, D. M. McCarty, and M. E. Thompson, Appl. Phys. Lett. **65**, 2922 (1994).
[7]L. Do, K. Kim, T. Zyung, and J. Kim, Appl. Phys. Lett. **70**, 3470 (1997).
[8]H. Sasabe and J. Kido, J. Mater. Chem. C **1**, 1699 (2013).
[9]I. R. De Moraes, S. Scholz, B. Lüssem, and K. Leo, Org. Electron. **12**, 341 (2011).
[10]S. Scholz, C. Corten, K. Walzer, D. Kuckling, and K. Leo, Org. Electron. **8**, 709 (2007).
[11]S. Scholz, K. Walzer, and K. Leo, Adv. Funct. Mater. **18**, 2541 (2008).
[12]Q. Wang and H. Aziz, Org. Electron. **26**, 464 (2015).
[13]Y. Zhang and H. Aziz, ACS Appl. Mater. Interfaces **8**, 14088 (2016).
[14]R. Coehoorn, H. Van Eersel, P. A. Bobbert, and R. A. J. Janssen, Adv. Funct. Mater. **25**, 2024 (2015).
[15]N. C. Giebink, B. W. D'Andrade, M. S. Weaver, P. B. MacKenzie, J. J. Brown, M. E. Thompson, and S. R. Forrest, J. Appl. Phys. **103**, 044509 (2008).
[16]Y. Zhang, J. Lee, and S. R. Forrest, Nat. Commun. **5**, 5008 (2014).
[17]Y. Shen and N. C. Giebink, Phys. Rev. Appl. **4**, 054017 (2015).
[18]Z. D. Popovic, H. Aziz, N. X. Hu, A. Ioannidis, and P. N. M. Dos Anjos, J. Appl. Phys. **89**, 4673 (2001).

[19]D. Y. Kondakov, W. C. Lenhart, and W. F. Nichols, J. Appl. Phys. **101**, 024512 (2007).
[20]S. Winter, S. Reineke, K. Walzer, and K. Leo, Proc. SPIE **6999**, 69992N (2008).
[21]K. W. Hershey and R. J. Holmes, J. Appl. Phys. **120**, 195501 (2016).
[22]D. Y. Kondakov, W. C. Lenhart, and W. F. Nichols, J. Appl. Phys. **101**, 024512 (2007).
[23]D. Y. Kondakov, J. R. Sandifer, C. W. Tang, and R. H. Young, J. Appl. Phys. **93**, 1108 (2003).
[24]M. A. Baldo, D. O'Brien, Y. You, A. Shoustikov, S. Sibley, M. E. Thompson, and S. R. Forrest, Nature **395**, 151 (1998).
[25]D. Y. Kondakov, W. F. Nichols, and W. C. Lenhart, SID Symp. Dig. Tech. Pap. **38**, 1494 (2007).
[26]Q. Wang and H. Aziz, Org. Electron. **12**, 1571 (2011).
[27]N. C. Erickson and R. J. Holmes, Adv. Funct. Mater. **23**, 5190 (2013).
[28]L. Huang, C. D. Park, T. Fleetham, and J. Li, Appl. Phys. Lett. **109**, 233302 (2016).
[29]C. Coburn and S. R. Forrest, Phys. Rev. Appl. **7**, 41002 (2017).
[30]J. Lee, C. Jeong, T. Batagoda, C. Coburn, M. E. Thompson, and S. R. Forrest, Nat. Commun. **8**, 15566 (2017).
[31]Q. Wang and H. Aziz, ACS Appl. Mater. Interfaces **5**, 8733 (2013).
[32]Q. Wang, B. Sun, and H. Aziz, Adv. Funct. Mater. **24**, 2975 (2014).
[33]J. Birnstock, T. Canzler, M. Hofmann, A. Lux, S. Murano, P. Wellmann, and A. Werner, J. Soc. Inf. Disp. **16**, 221 (2008).
[34]F. Xu, K. W. Hershey, R. J. Holmes, and T. R. Hoye, J. Am. Chem. Soc. **138**, 12739 (2016).
[35]C. Coburn, J. Lee, and S. R. Forrest, Adv. Opt. Mater. **4**, 889 (2016).
[36]J. Lee, H.-F. Chen, T. Batagoda, C. Coburn, P. I. Djurovich, M. E. Thompson, and S. R. Forrest, Nat. Mater. **15**, 92 (2015).
[37]S. Yi, J. H. Kim, Y. J. Cho, J. Lee, T. S. Choi, D. W. Cho, C. Pac, W. S. Han, H. J. Son, and S. O. Kang, Inorg. Chem. **55**, 3324 (2016).
[38]S.-K. Kim, B. Yang, Y. Ma, J.-H. Lee, and J.-W. Park, J. Mater. Chem. **18**, 3376 (2008).